

## **General Disclaimer**

### **One or more of the Following Statements may affect this Document**

- This document has been reproduced from the best copy furnished by the organizational source. It is being released in the interest of making available as much information as possible.
- This document may contain data, which exceeds the sheet parameters. It was furnished in this condition by the organizational source and is the best copy available.
- This document may contain tone-on-tone or color graphs, charts and/or pictures, which have been reproduced in black and white.
- This document is paginated as submitted by the original source.
- Portions of this document are not fully legible due to the historical nature of some of the material. However, it is the best reproduction available from the original submission.



Technical Memorandum 82040

# SEASAT ALTIMETER HEIGHT CALIBRATION

(NASA-TM-82040) SEASAT ALTIMETER HEIGHT  
CALIBRATION (NASA) 42 p HC A03/MF A01

N81-19526

CSCL 05B

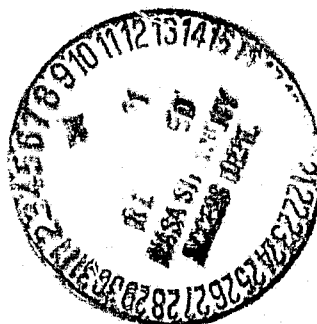
Unclassified  
G3/43 18820

R. Kolenkiewicz  
C. F. Martin

MARCH 1981

National Aeronautics and  
Space Administration

Goddard Space Flight Center  
Greenbelt, Maryland 20771



TM 82040

**SEASAT ALTIMETER HEIGHT CALIBRATION**

Ronald Kolenkiewicz  
Geodynamics Branch  
National Aeronautics and Space Administration  
Goddard Space Flight Center  
Greenbelt, Maryland 20771

Chreston F. Martin  
EG&G Washington Analytical Services Center, Inc.  
6801 Kenilworth Avenue  
Riverdale, Maryland 20840

March 1981

**GODDARD SPACE FLIGHT CENTER**  
Greenbelt, Maryland 20771

## SEASAT ALTIMETER HEIGHT CALIBRATION

Ronald Kolenkiewicz  
Geodynamics Branch  
National Aeronautics and Space Administration  
Goddard Space Flight Center  
Greenbelt, Maryland 20771

Chreston F. Martin  
EG&G Washington Analytical Services Center, Inc.  
6801 Kenilworth Avenue  
Riverdale, Maryland 20840

### ABSTRACT

The Seasat altimeter has been calibrated for height bias using four overflight passes of Bermuda which were supported by the Bermuda laser. The altimeter data was corrected for: tides, using recorded tide gauge data; propagation effects, using meteorological data taken around the time of each pass; acceleration lag; and sea state bias, including both surface effects and instrumental effects. Altimeter data for each of the four passes was smoothed and extrapolated across the island. Interpolation between passes then produced an equivalent altimeter measurement to the geoid at the laser site, so that the altimeter bias could be estimated without the use of a geoid model. The estimated height bias was  $0.0 \pm 0.07$  m.

PRECEDING PAGE BLANK NOT FILMED

## SEASAT ALTIMETER HEIGHT CALIBRATION

### INTRODUCTION

In support of altimeter height bias calibration, the Seasat orbit was adjusted on September 10, 1978, to obtain a repeating (every 43 revolutions, approximately 3 days) ground-track which passes as close as possible to the Bermuda laser site. Between September 10 and the spacecraft power failure on October 10, 1978, there were 10 North to South Bermuda overflights with the ground-tracks shown in Figure 1. All passes were supported by the NASA Spacecraft Tracking and Data Network (STDN), with four passes supported by the Bermuda laser. These laser supported passes provide the primary information for absolute bias calibration and stability analysis of the Seasat Altimeter. The remaining six passes are useful, however, for analyzing errors in smoothed and extrapolated altimeter data across Bermuda. With extensive analysis, these passes could also be used to help develop a geoid model in the vicinity of the Bermuda laser and thus simplify future altimeter calibration efforts.

### CALIBRATION TECHNIQUE

The Seasat altimeter calibration technique is based on GEOS-3 experience (Martin and Butler, 1978; Martin and Kolenkiewicz, 1980) and was outlined in the Seasat Calibration Plan (Martin, 1978). It consists basically of the use of altimeter passes over Bermuda with laser tracking support (for accurate orbit height determination) and altimeter tracking, on both sides of Bermuda, which can be extrapolated to obtain equivalent sea surface height measurements on the island itself. The objective is to create an equivalent altimeter measurement over the laser tracking site which can be related to sea surface heights several kilometers away from the island with an accuracy compatible with a total calibration error budget of  $\sim 7$  cm\*. Available geoid models cannot provide the desired

---

\*A bias of this accuracy can then be used to produce corrected altimeter data which will have the proverbial 10 cm accuracy (Martin, 1977).

accuracy, so it is necessary to use the altimeter data itself to provide the water-land extrapolation. No geoid model was used in the calibration analyses discussed below.

To demonstrate the elements of the overhead calibration technique, consider the basic calibration geometry as shown in Figure 2. Assuming a pass directly over a laser tracking station with continuous laser and altimeter tracking, the measurements directly over the tracking station can be used for bias estimation by equating the altimeter measurement, corrected to the ellipsoid, with the laser measurement also corrected to the ellipsoid. Equating the two measurements shown in Figure 2,

$$h_a = b + h_t + \delta h + h_{ga} = h_{gs} + h_m + R \quad (1)$$

where

- $h_a$  = measured altimeter height above the sea surface corrected for instrumental and atmospheric propagation effects and spacecraft center of mass offset,  
 $b$  = bias in the altimeter measurement,  
 $h_t + \delta h$  = tide measurement as determined by the tide gauge at the time of the altimeter pass. This measurement includes non-tidal temporal sea surface variations.  
 $h_{ga}$  = geoid height at the altimeter subsatellite point,  
 $R$  = measured distance from the laser tracking station to the laser corner cube reflectors corrected for instrumental and atmospheric propagation effects and spacecraft center of mass offset,  
 $h_m$  = height of the tracking station above mean sea level (the geoid) at the tracking station.  
 $h_{gs}$  = geoid height at the tracking station.

The altimeter measurement bias can thus be determined, using Equation (1), from the expression:

$$b = h_a + h_t + \delta h + h_{ga} - [R + h_{gs} + h_m] \quad (2)$$

The terms in brackets on the right-hand side of Equation (2) constitute the ellipsoidal height normally calculated in orbit determination programs, while the terms outside the brackets give the

ellipsoidal height based on the altimeter measurement, a measured tide, and a geoid model. The right-hand side is thus the "observed" minus "computed" measurement, normally referred to as the measurement residual. The residual can be calculated whether the satellite is directly over the laser site or not, although only at the direct overhead point will the two geoid heights be identical and thus cancel.

In practice, the altimeter cannot accurately track directly over the laser site because of land in the altimeter footprint, and the laser does not track directly overhead because its Az-EI mount cannot follow the high azimuth rates in the vicinity of the point of closest approach (PCA). However, the latter is not a problem because an accurate overhead orbit can be estimated with a gap in the data around the PCA.

After deleting measurement points which have been significantly influenced by the presence of land in the footprint, the altimeter data can be smoothed across Bermuda to obtain extrapolated altimeter residuals at the groundtrack points of closest approach to the laser site. These extrapolated residuals can then be used along with the laser orbit and various corrections to obtain the altimeter height bias. Details and results are described below.

#### ORBIT DETERMINATION

The critical tracking data for orbit determination is Bermuda tracking data on the overflight pass. For all calibration passes having Bermuda laser support, data was taken both before and after PCA and simulations have shown that the quantity of data taken was adequate to obtain orbit height accuracies at the laser site of 2-3 cm, based on an observed laser noise level of 5-8 cm and assumed laser bias well below this level.

For supporting tracking data, calibrations area laser data was used when adequate, and S-Band data was added when there was insufficient laser support. The stations used are shown in Table 1. The calibration orbits for September 13 and September 22 were estimated using laser data on the

overflight pass plus the following pass. For September 16 and October 1, laser data were supplemented by S-Band data from Merritt Island, Bermuda, and Santiago on the overflight pass and adjacent revolutions. In all cases, the laser data from Bermuda were weighted with a standard deviation of 10 cm, while all other laser data were weighted with a standard deviation of 1 m, thus allowing the orbit height over Bermuda to be determined predominantly by the Bermuda laser.

The only station position coordinate which strongly effects the estimated heights is the Bermuda laser ellipsoid height, for which a value of -26.53 m was used. Since the surveyed mean sea level (MSL) height of the Bermuda laser is 13.44 m, a geoid height ( $h_{gs}$  in Figure 2) of -39.97 m is implied.

#### ANALYSIS OF BERMUDA OVERFLIGHT DATA

Before using the altimeter data smoothing program to extrapolate across Bermuda, it is necessary to first decide which data points should be weighted and which should be edited. Figure 3 shows the groundtracks of the four Bermuda overflights for which Bermuda laser data was taken, and indicates the groundtrack locations for the weighted and edited points. The editing of points was based on the examination of Automatic Gain Control (AGC) data (shown in Figure 4), on the examination of Significant Wave Height (SWH) data (shown in Figure 5), on the examination of 10-second waveform data, and on the altimeter effective footprint and lag characteristics. In addition, the altimeter residuals were examined after smoothing to see that no anomalous points remained.

In general, the edited points in Figure 4 correspond to anomalously high AGC values which would be expected from the presence of significant land in the altimeter footprint. For September 22, the AGC is also high approaching Bermuda. As seen in Figure 5, the SWH is very low (<1m) during this period. In addition, the altitude data has short wavelength fluctuations several seconds before the groundtrack reaches Bermuda (see Figure 8). However, AGC has only a second order effect on altitude, and the smoother should effectively damp out the oscillations that may be due to a near specular ocean return.

In interpreting the SWH data, it should be noted that the Seasat altimeter tracker makes use of return signal up to 92 nsec after the time of the nominal sub-satellite return. This 92 nsec delay corresponds to a surface distance of some 6.6 km, or approximately 1 second of satellite ground-track. The groundtrack points in Figure 3 show that each of the laser supported passes reaches land about 0.4 seconds prior to the closest approach to the laser site, so there can be no direct land influence on altimeter heights prior to 1.4 seconds before the closest approach to laser point. For each pass, data has been accepted some 0.3 - 0.4 seconds of data past this first influence point on the basis that (a) the initial land influence is weak because of the antenna beam pattern and the low tracker sensitivity to slight perturbations in the trailing edge of the return pulse, and (b) the 0.8 second time constant of the tracker. The additional 3-4 data points have good residual patterns (compared to the smoothed points) and do not have waveforms that are visibly affected by land when examined at the 10/second data rate.

Based on the SWH data in Figure 5, the influence of Bermuda is visible at least 2 seconds prior to the laser crossing. Since the direct influence of land cannot occur this early, we must have some other phenomenon which modifies the return waveform other than land. Since the SWH would be expected to be lower for the shallow water northeast of Bermuda, the initial SWH measurement can be interpreted as due to a real SWH decrease. At the SWH minimum, however, land has begun to influence the waveform and the correspondence of the altimeter measured waveheights to actual SWH's is at best tenuous.

After the island has been crossed, the editing adopted is rather conservative. For the weighted data points, both the AGC and SWH have nearly achieved stable values.

Figures 6-9 show the raw and smoothed altimeter residuals around Bermuda for the four laser supported calibration passes, with the time origin the time of closest approach to the laser. The residuals were computed using the "observed" minus "computed" ellipsoidal heights, analogous to Equation (2), but without applying the geoid  $h_{ga}$  to the altimeter data and without yet applying all

the desired altimeter corrections. The smoothing was performed using the ALTKAL smoother (Fang and Amann, 1977). For at least two of the passes, September 13 and September 22, the editing after Bermuda appears to have been overly conservative and almost a second of good data may have been edited. For September 16, however, none of the edited points past Bermuda are consistent with the smoothed residuals.

## DATA CORRECTIONS

Some simplifications have been made in Equation (2), primarily in the  $h_a$  term. In practice, this quantity must be obtained from the measured altitude data, corrected for propagation effects, instrumentation response characteristics, sea state effects, and spacecraft delays and antenna offsets. These corrections are summarized in Table 2 for the four laser supported calibration passes. The sea state bias is one of the most uncertain corrections because the process is presently so poorly understood. However, it now seems clear that there are at least two effects here which are sea state dependent and which we have combined under sea state "bias":

1. Surface effects. Since microwave scattering cross sections tend to be higher in wave troughs than for wave crests, the electronic mean sea surface is shifted downward from the geometric mean sea surface. The amount of the shift is a function of SWH and probably other surface properties. The latter are at least partially characterized by height skewness. According to Jackson (1979), sea state bias may be approximated by the product of RMS waveheight and height skewness. For "typical" values of height skewness of 0.2, this bias reduces to 5% of SWH. On the basis of Surface Contour Radar measurements, Walsh (1980) considers a 1-2% figure to be more appropriate than 5%. A dependence of bias on surface properties other than SWH has been confirmed by Walsh. He found essentially zero bias for a 5.5m swell dominated sea.
2. Instrumental Effects. Since the Seasat altimeter transmitted pulse shape differs significantly from that assumed in its on-board processing (a Gaussian), an error is induced in the

on-board height computations. No correction is made for this error source in the normal ground processing.\* Hayne (1980) has computed height corrections\*\* due to pulse shape as a function of SWH and height skewness. For significant wave heights of 1-3 m that are of interest for the calibration passes, Hayne's altitude errors are on the order of 6-10 cm. The correction is always negative and is an increasing function (in magnitude) of SWH as is the sea state bias due to surface properties.

Based on the current state of theoretical, experimental, and simulation results, the existence of a sea state bias due both to surface properties and to instrumental/processing effects is essentially incontestable. Accordingly, it is assumed that corrections should be made for both types of errors, although uncertainties will be high due to the tentative state of current correction models. Hayne's results (Hayne, 1980) have been used for the instrumental effects and the upper bound of Walsh's estimate (2% of SWH) has been used for the sea state bias due to surface effects. Table 3 summarizes the correction computation.

#### DATA CONSISTENCY

Although they do not by themselves constitute direct accuracy checks, there are several consistency tests which can be performed on the altimeter data and from which accuracy confidence may be gained. Two of the tests also include orbit height as an accuracy variable.

---

\*In addition to a Gaussian pulse, the on-board processing also assumes zero off-nadir angle. A correction is computed in ground processing (at JPL). For low sea states, this effect is typically on the order of 1-2 cm. Because of its low magnitude, a correction for this effect has not been applied in the calibration data processing.

\*\*Strictly speaking, the tracker utilized in Hayne's computations is not the same as that used in the SEASAT on-board processor. It is the opinion of the authors that the distinction is not significant for computing the effects of the non-Gaussian pulse. But it should be noted that Hayne's Gaussian tracker and the on-board tracker's response to a Gaussian may also have a bias between them. Such a bias probably exists, but it is academic except to the extent that it is sea state dependent, since a bias for the on-board tracker is being estimated.

First, consider the smoothed corrected residual profiles\* for the four laser supported calibration passes shown in Figure 10. The negatives of these residuals are the geoid profiles. Between -1 second and almost 3 seconds, these curves are based on extrapolations. On the assumption of a linear geoid variation in the direction perpendicular to the groundtracks (to be validated below), the separation between passes should be proportional to the product of groundtrack separation and geoid slope. Past Bermuda, where the geoid slopes are high, the passes maintain separations which are consistent with a low level of data errors being propagated through the ALTKAL smoother. About 3 seconds prior to Bermuda, the profiles cross, indicating a zero geoid slope (perpendicular to the passes) in this region. On the basis of our geoid knowledge, this zero slope is acceptable. However, prior to -3 seconds, the relative residual separations are not consistent. With the geoid slope change at -3 seconds, the September 16 pass should fall below the October 1 pass during the -5 to -3 second period, instead of being above by about 6 cm. But this discrepancy is consistent with the ~10 cm individual pass uncertainties discussed below.

On the other hand, the September 22 pass appears to have definitely anomalous behavior in the -5 to -3 second period. This has already been noted in the AGC behavior in Figure 4. The altitude residuals for the pass (Figure 8) also indicate anomalous behavior. But the September 22 residuals seem to settle down about one second prior to the land crossing, and the pass is otherwise consistent with the other three calibration passes, so it has been used as a part of the height bias calibration.

Next consider the agreement of the calibration passes with the two South-North passes that have been shown in Figures 1 and 3. Since these passes do not have laser support, they can be used only to demonstrate consistency of the calibration passes. Due to the short distances involved, it is expected that the South-North passes would have relative errors (in the smooth residuals) only at the 1-2 cm level between crossings of the September 13 and October 1 passes. The rms differences

---

\*These are the smoothed altimeter residuals of Figures 6-9 with the corrections of Table 2 applied.

shown in Tables 3 and 4 of 3 cm and 5 cm respectively, are thus indicative of the pass to pass variation in measured geoid heights around Bermuda for a laser supported calibration pass.

It should be noted that the above comparisons are affected by smoothing errors, orbit errors, and errors in all the data corrections (including tides, refraction, and sea state bias.) Except for the possibility that some of the error sources have systematic components, and the fact that the calibration point of interest is further into the extrapolation data period, it follows that the  $1\sigma$  accuracy for an individual pass is  $\sim 4$  cm.

Finally, note from the groundtrack shown in Figure 1 that there are several passes which so closely overlap that the separate groundtracks are not discernable from the plots. Differences between the smoothed residuals for various pairs of such passes indicate the characteristics and magnitudes of errors in the smoothed residuals across Bermuda. Figures 11-14 show four pairs of such differences, based on the October 1 calibration pass and four passes which did not have laser support: September 25, September 28, October 4 and October 7. The differences would be expected to be oscillatory, with typical periods on the order of 4 seconds (corresponding to the 25 km correlation length used in the smoother) and three of the four sets of differences do indeed show such general behavior. Based on the average rms from the four figures of 6.3 cm and considering that each plot is the difference of independent qualities, an estimate of 4.5 cm is obtained for the  $1\sigma$  error due to the propagation of measurement noise into the smoother.

## BIAS ESTIMATION AND ANALYSIS

Table 6 lists the residuals for each of the calibration passes at the closest approach to the laser site. These residuals then need to be extrapolated to the latitude of the laser site in order to obtain the equivalent residual for a point at which the geoid height is "known". For this extrapolation, it is assumed that the geoid varies linearly between the September 13 and October 1 passes. This assumption may be justified by noting that South-North passes in the vicinity of the laser on July 16 and August 2 have residuals which are closely approximated by straight lines. As shown in

Figures 15 and 16, the deviations from a straight line fit are at the sub-centimeter level between crossings of the September 13 and October 1 passes.

The data from Table 6 is plotted in Figure 17, with error bars as computed in Table 7. The numbers given in Table 7 are considered to be realistic  $1\sigma$  error estimates for the various error sources. Included is an uncertainty in an acceleration correction which will be added below. The uncertainty is not in the correction model but in the acceleration computation which must be made using smoothed data. On the other hand, the uncertainties in the sea state bias corrections are primarily due to correction model uncertainties, although there is also some problem in obtaining appropriate sea state values. The tide correction uncertainties are due to a number of potential error sources, whose magnitudes have been analyzed by NOAA (Diamonte, et al., 1981). Error estimates for September 16 are larger than for the other three passes due to the higher winds (13 knots) and the associated wind setup effects.

No timing error contributions are included in the uncertainties listed in Table 7. All passes were processed using the timing algorithms given by Hancock et al. (1980), although admittedly the algorithm has not been applied in one step (part was applied at JPL and part was applied at GSFC.) There is strong evidence for believing that all significant timing problems have been found and corrected. Various crossing arc analyses, some of which were based on short arc results and some of which were based on global data sets (Schutz, et al., 1981), have given results which are in agreement to within the theoretically computed timing algorithm. In addition, the theoretical algorithm was the result of an extensive analysis of the on-board data processing and time tagging.

A weighted least squares fit to the data points is shown in Figure 17, using weights based on the total sigmas from Table 7 and the sea state bias errors considered to be totally correlated (consistent with the errors being due to model errors). The residual at the laser latitude is  $39.90 \pm 0.07$  m. It may be noted that a constant weighting of the data points also gives 39.90 m at the laser latitude, so the choice of weighting does not significantly influence the estimated bias value.

One final correction which has not yet been applied to the altimeter residuals is the affects of acceleration lag. The acceleration lag error is  $\Delta \text{accel}/K_A$ , where  $K_A = 6.5/\text{sec}^2$ . For all four passes at the closest approach to laser point, the lag correction is approximately 7 cm. Adding this correction and the geoid height at the laser to the residual obtained from Figure 17 have:

Residual at laser site		39.90 m
+ Acceleration lag correction		0.07 m
+ Geoid height at laser site		-39.97 m
Bias	=	0.00 m

It is thus concluded that, if the Seasat altimeter data is accurately corrected for propagation effects, and is corrected for sea state bias with a procedure equivalent to the one used in the analysis, the appropriate bias for the altimeter is  $0.0 \pm 0.07$  m. Assuming a data noise level of  $\sim 7$  cm, which was in fact observed at even the 10/sec data rate for all the calibration passes, the Seasat altimeter is indeed a 10 cm altimeter.

#### SUMMARY AND CONCLUSIONS

Extensive analysis of Seasat altimeter data for the four laser supported satellite passes across Bermuda have led to a bias estimate of  $0.00 \pm 0.07$  m, with measurement noise and sea state bias uncertainty the dominant contributors to the estimated bias sigma. In the altimeter data processing, a sea state dependent correction (varying between 5 and 16 cm for the four calibration passes) is applied, and it is recommended that such a correction be utilized by all data users desiring to achieve 10 cm data accuracy.

## REFERENCES

- Diamonte, J. M., B. C. Douglas, D. L. Porter, and R. P. Masterson, Jr., "The Surface Truth for the Seasat Calibration Experiment", Submitted to JGR for publication.
- Fang, B. R., and D. W. Amann, "ALTKAL - An Optimum Linear Filter for GEOS-3 Altimeter Data," NASA CR-141429, August 1977.
- Hancock, D. W., R. G. Forsythe, and J. Lorell, "Seasat Altimeter Sensor File Algorithms," IEEE Jr. Oceanic Engr. OE-5, 93-99, 1980.
- Hayne, G. S., "Wallop's Waveform Analysis of Seasat-1 Radar Altimeter Data," NASA CR-156869, July 1980.
- Jackson, F. C., "The Reflection of Impulses from a Nonlinear Random Sea," JGR 84, 4939-4943, 1979.
- MacArthur, J. L., "Seasat-A Radar Altimeter Design Description," APL/JHU, SDO-5232, Applied Physics Laboratory, Laurel, Md., November 1978.
- Martin, C. F., "Altimeter Error Sources at the 10 cm Performance Level," NASA CR-141420, April 1977.
- Martin, C. F., "Calibration Plan for the Seasat Altimeter," EG&G Washington Analytical Services Center Report PSD02-78, January 1978.
- Martin, C. F., and M. L. Butler, "Calibration Results for the GEOS-3 Altimeter," NASA CR-141430, September 1977.
- Martin, C. F., and R. Kolenkiewicz, "Calibration Validation for the GEOS-3 Altimeter," NASA TM 80710, June 1980.

Mofjeld, A. O., "Empirical Model for Tides in the Western North Atlantic Ocean," NOAA Technical Report ERL 340-AOML-19, October, 1975.

Schutz, B. E., B. D. Tapley, J. G. Marsh, R. G. Williamson "The Time Bias in the Altimeter Measurement," Submitted to JGR for publication.

Walsh, E. J., NASA/WFC, Private Communication, 1980.

## ACKNOWLEDGEMENTS

The authors would like to acknowledge the assistance provided by a number of individuals, not all of which have been explicitly referenced. W. F. Townsend and D. W. Hancock assisted in the assessment of data validity around Bermuda, and also provided explanations of the nature of various instrument corrections. George Hayne provided results and discussions of his waveform analysis of Seasat data, including the instrument correction that has been used in the bias estimation. E. J. Walsh for providing the results of his sea state bias analyses, as well as assessing the results of other investigations. All of the above individuals are with NASA Wallops Flight Center. Barbara Putney and George Wyatt of NASA Goddard Space Flight Center also provided valuable assistance in solving various data processing problems.

TABLE 1. TRACKING SUPPORT USED FOR CALIBRATION ORBIT ESTIMATION

Date of Pass	9/13/76	9/16/76	9/22/76	10/1/76
Data Start Time	2 <sup>h</sup> 58 <sup>m</sup> 43 <sup>s</sup>	1 <sup>h</sup> 50 <sup>m</sup> 40 <sup>s</sup>	3 <sup>h</sup> 38 <sup>m</sup> 1 <sup>s</sup>	3 <sup>h</sup> 0 <sup>m</sup> 50 <sup>s</sup>
Data End Time	4 <sup>h</sup> 43 <sup>m</sup> 47 <sup>s</sup>	4 <sup>h</sup> 59 <sup>m</sup> 40 <sup>s</sup>	5 <sup>h</sup> 21 <sup>m</sup> 57 <sup>s</sup>	6 <sup>h</sup> 6 <sup>m</sup> 30 <sup>s</sup>
Laser Support on Overflight Pass	Bermuda, Grand Turk	Bermuda, Grand Turk	Bermuda, Goddard	Bermuda, Grand Turk
Laser Support on Pass Following Overflight	Patrick	None	Patrick, Goddard	None
S-Band Stations Used	None	Santiago, Merritt Island, Bermuda	None	Santiago, Merritt Island, Bermuda

TABLE 2. BERMUDA LASER SUPPORTED CALIBRATION PASS CORRECTIONS

(meters)

Date in 1978 (M/D)	9/13	9/16	9/22	10/1	Comments
TIDE CORRECTION	0.02	0.05	0.04	0.24	Based on smoothed tide gauge readings. Numbers are differences between tide gauge and Mofjeld tide model (Mofjeld)
DRY TROPOSPHERE	-2.33	-2.31	-2.34	-2.32	
WET TROPOSPHERE	-0.25	-0.19	-0.26	-0.33	Based on radiosonde data, except for Sept. 13 which was based on surface meteorological data
IONOSPHERE	-0.02	-0.02	-0.02	-0.02	
CENTER OF GRAVITY	6.04	6.04	6.04	6.04	Includes pre-launch calibration delays
SEA STATE BIAS	-0.11	-0.16	-0.05	-0.13	See Table 3
TOTAL	3.35	3.41	3.41	3.48	

TABLE 3. SIGNIFICANT WAVE HEIGHTS AND SEA STATE BIASES  
FOR CALIBRATION PASSES

Date M/D	SWH* at -1.25 seconds	Non-Gaussian Instrument Correction**	Sea State Bias at 2% of SWH	Total Sea State Bias
9/13	1.8 m	-0.07 m	-0.04 m	-0.11 m
9/16	3.1 m	-0.10 m	-0.06 m	-0.16 m
9/22	0.7 m	-0.04 m	-0.01 m	-0.05 m
10/1	1.8 m	-0.09 m	-0.04 m	-0.13 m

\*Includes off-nadir pointing correction

\*\*From Hayne (1980), Figure 10

TABLE 4. TIMES AND RESIDUALS FOR JULY 16 INTERSECTIONS

Date of Pass in 1978 (M/D)	Calibration Pass Residual* (m)	Calibration Pass Time (H:M:S)	July 16 Residual (m)	Residual Difference July 16 Minus Calibration Pass (m)	Corrected July 16 Residual** (m)	Calibration Pass Residual Minus Corrected July 16 Residual
9/13	39.92	03:02:06.5208	36.73	-3.19	39.96	-0.04
9/16	39.91	03:14:52.1828	36.66	-3.25	39.89	0.02
9/22	39.77	03:40:23.1420	36.55	-3.22	39.78	-0.01
10/1	39.75	04:18:37.1345	36.49	-3.26	39.72	0.03
			Mean	-3.23	RMS =	0.03

\*Values corrected using Table 2.

\*\*Corrected to agree with Bermuda Laser supported calibration passes by subtracting the mean residual differences from the previous column.

TABLE 5. TIMES AND RESIDUALS FOR AUGUST 2 INTERSECTIONS

Date of Pass in 1978 (M/D)	Calibration Pass Residual* (m)	Calibration Pass Time (H:M:S)	Aug. 2 Residual (m)	Residual Difference Aug. 2 Minus Calibration Pass (m)	Corrected Aug. 2 Residual** (m)	Calibration Pass Residual Minus Corrected Aug. 2 Residual
9/13	41.54	03:02:09.5754	40.53	-1.01	41.52	0.02
9/16	41.33	03:14:55.2373	40.36	-0.97	41.35	-0.02
19 9/22	41.09	03:40:26.1965	40.04	-1.05	41.03	0.06
10/1	40.78	04:18:40.1892	39.85	-0.93	40.84	-0.06
			Mean	-0.99	RMS =	0.05

\*Values corrected using Table 2.

\*\*Corrected to agree with Bermuda Laser supported calibration passes by subtracting the mean residual difference from the previous column.

TABLE 6. TIMES, LATITUDES, AND RESIDUALS FOR CLOSEST APPROACH  
TO LASER

Date of Pass in 1978 (M/D)	Time (H:M:S)	Latitude (Deg.)	Corrected Residual* (m)
9/13	03:02:06.9541	32.3520	39.93
9/16	03:14:52.6862	32.3553	39.88
9/22	03:40:23.7821	32.3615	39.73
10/1	04:18:37.8574	32.3653	39.66

\*Values corrected using Table 2.

TABLE 7. UNCERTAINTIES IN CLOSEST APPROACH HEIGHTS FOR LASER SUPPORTED CALIBRATION PASSES

Date in 1978 (M/D)	(meters)			
	9/13	9/16	9/22	10/1
<b>Residual:</b>				
Orbit	0.03	0.03	0.03	0.03
Measurement Noise Propagated Through Smoother	0.05	0.05	0.05	0.05
Title Correction	0.03	0.04	0.03	0.03
Dry Troposphere	0.02	0.02	0.02	0.02
Wet Troposphere	0.02	0.02	0.02	0.02
Ionosphere	0.01	0.01	0.01	0.01
Acceleration Correction	0.02	0.02	0.02	0.02
Sea State Bias	0.05	0.08	0.03	0.05
Total Uncertainty (RSS)	0.09	0.11	0.08	0.09

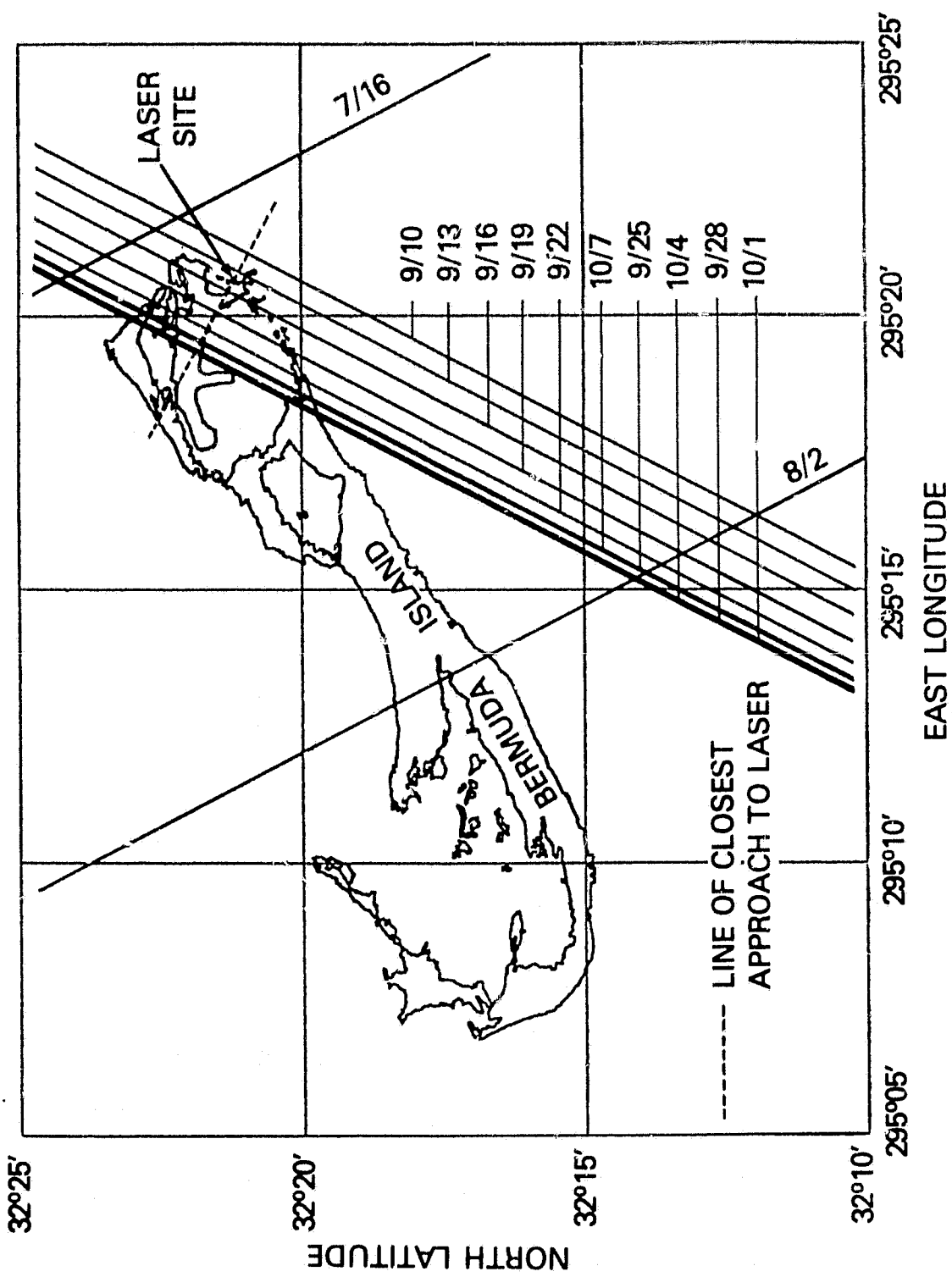


Fig. 1. Groundtracks for Bermuda calibration overflights.

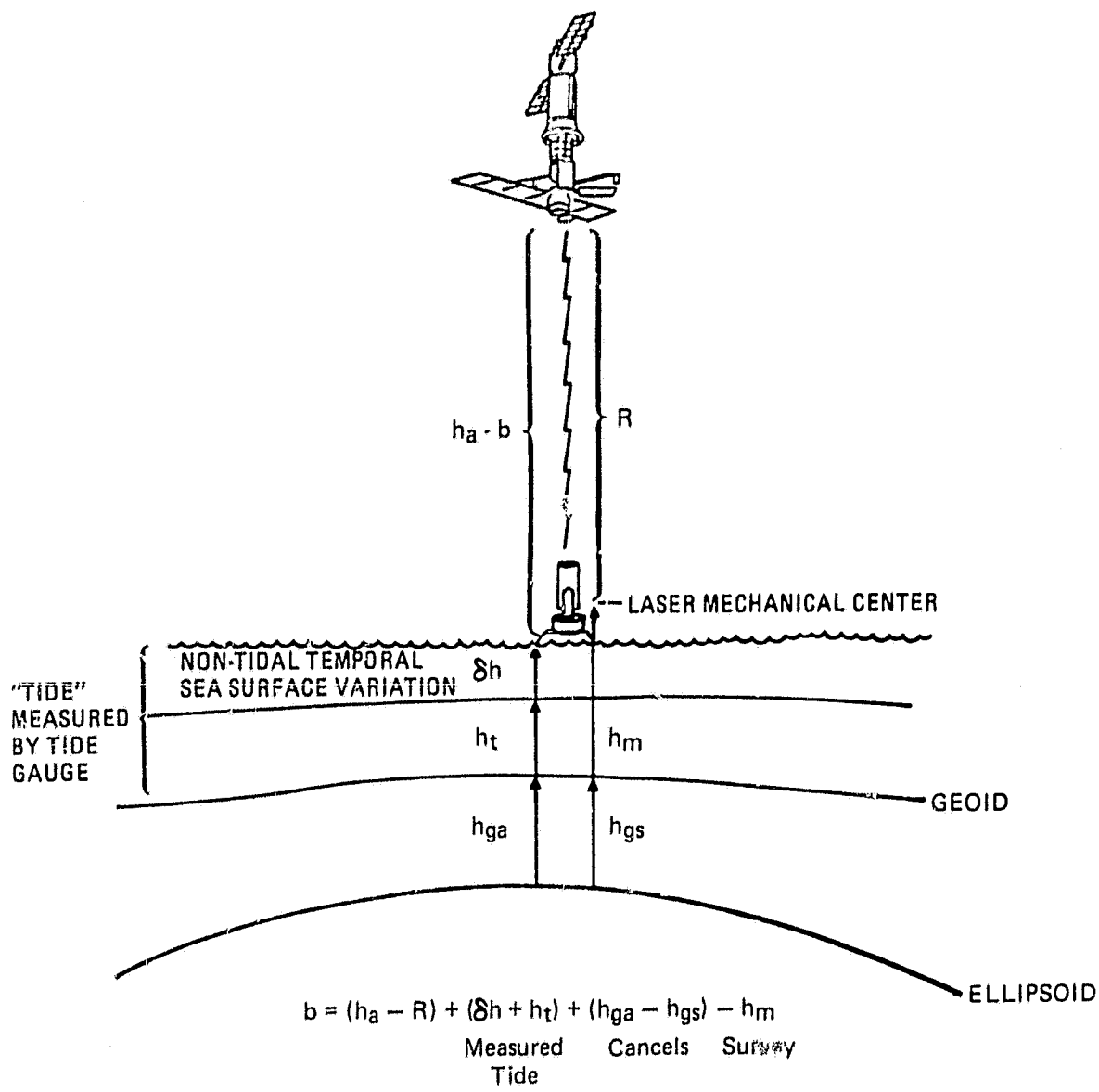


Fig. 2. Calibration geometry using overhead pass.

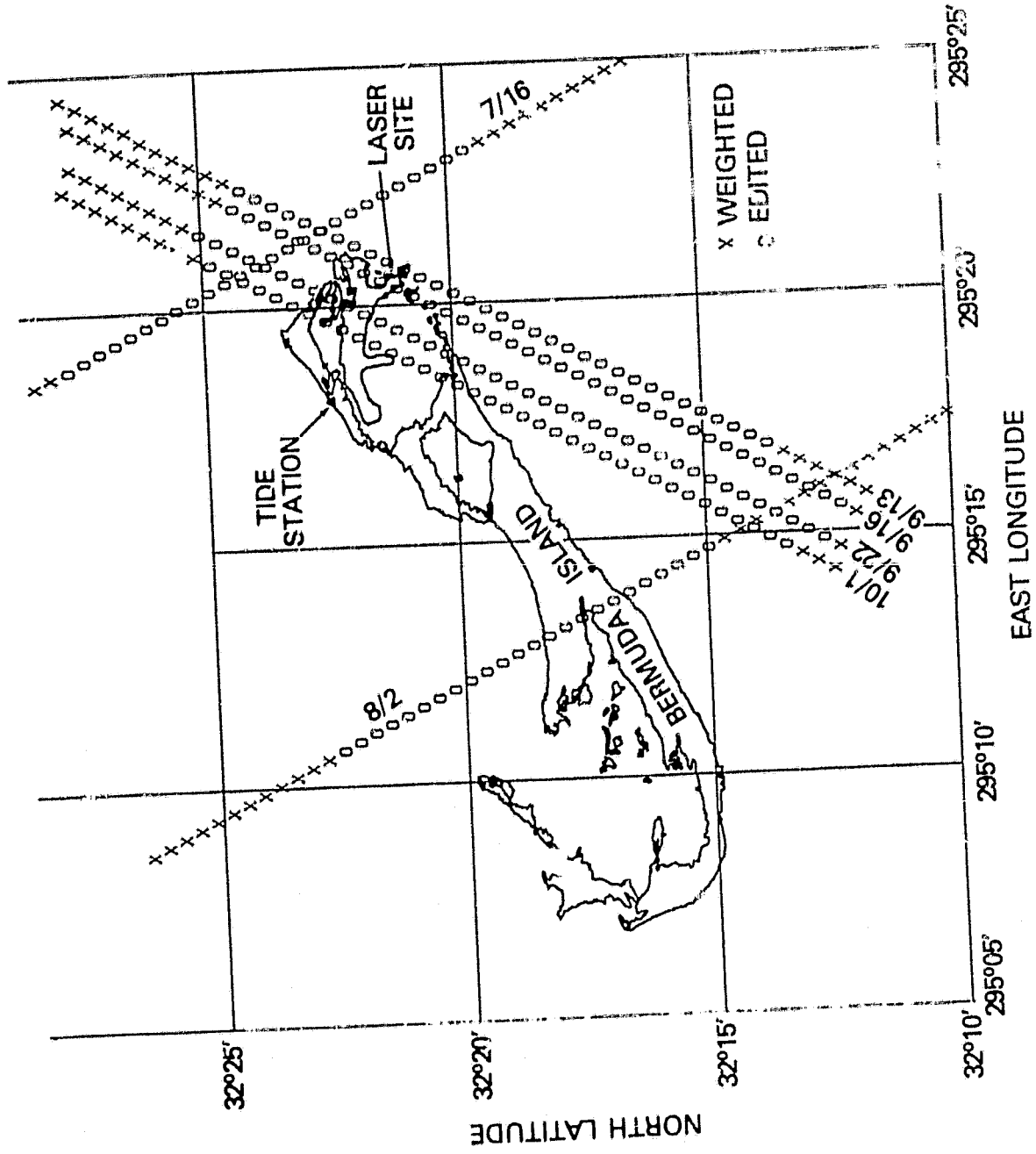


Fig. 3. Groundtracks for four laser-supported north to south Bermuda overflights showing edited data segments.

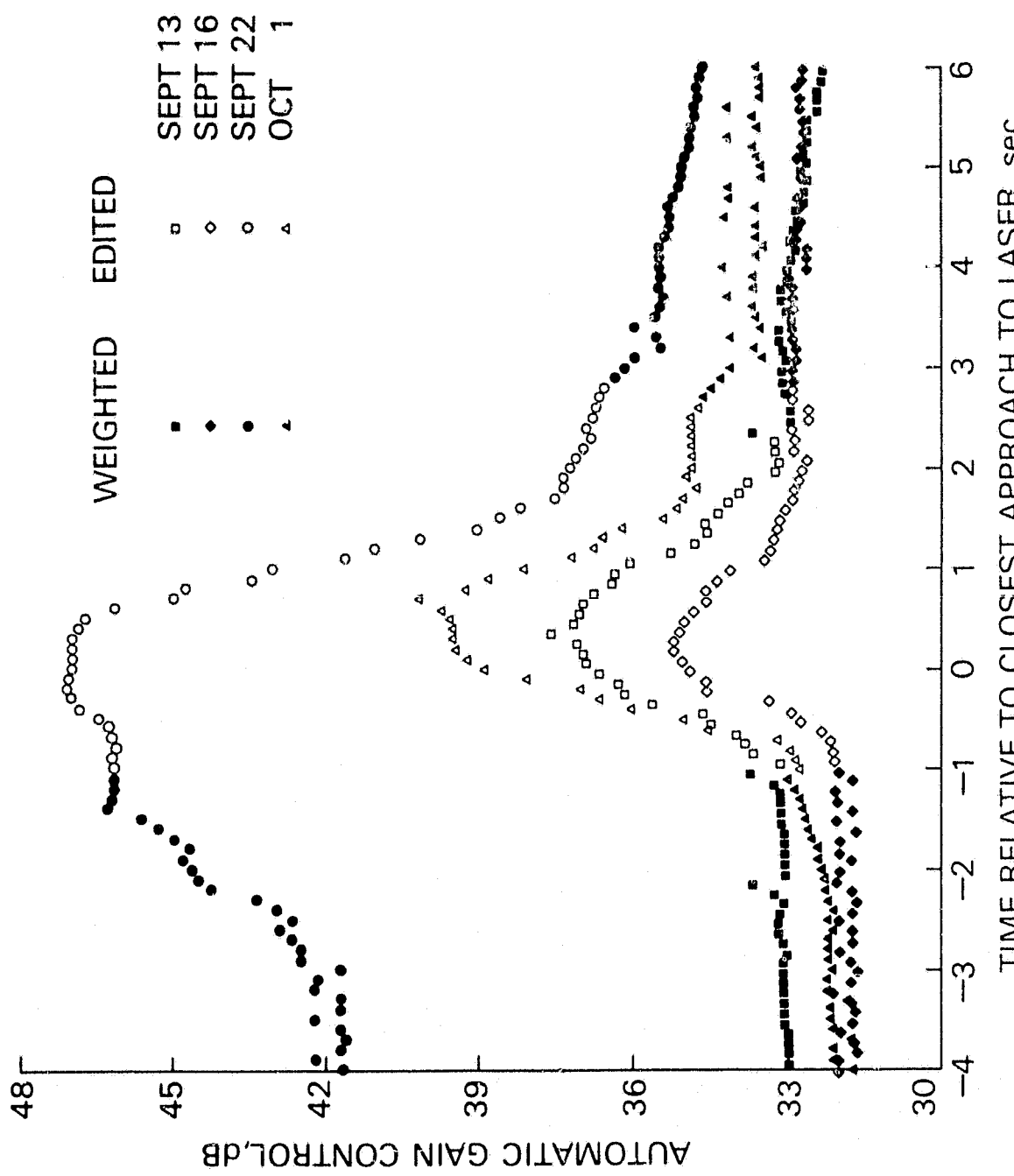


Fig. 4. Automatic gain control (AGC) data in the vicinity of Bermuda.

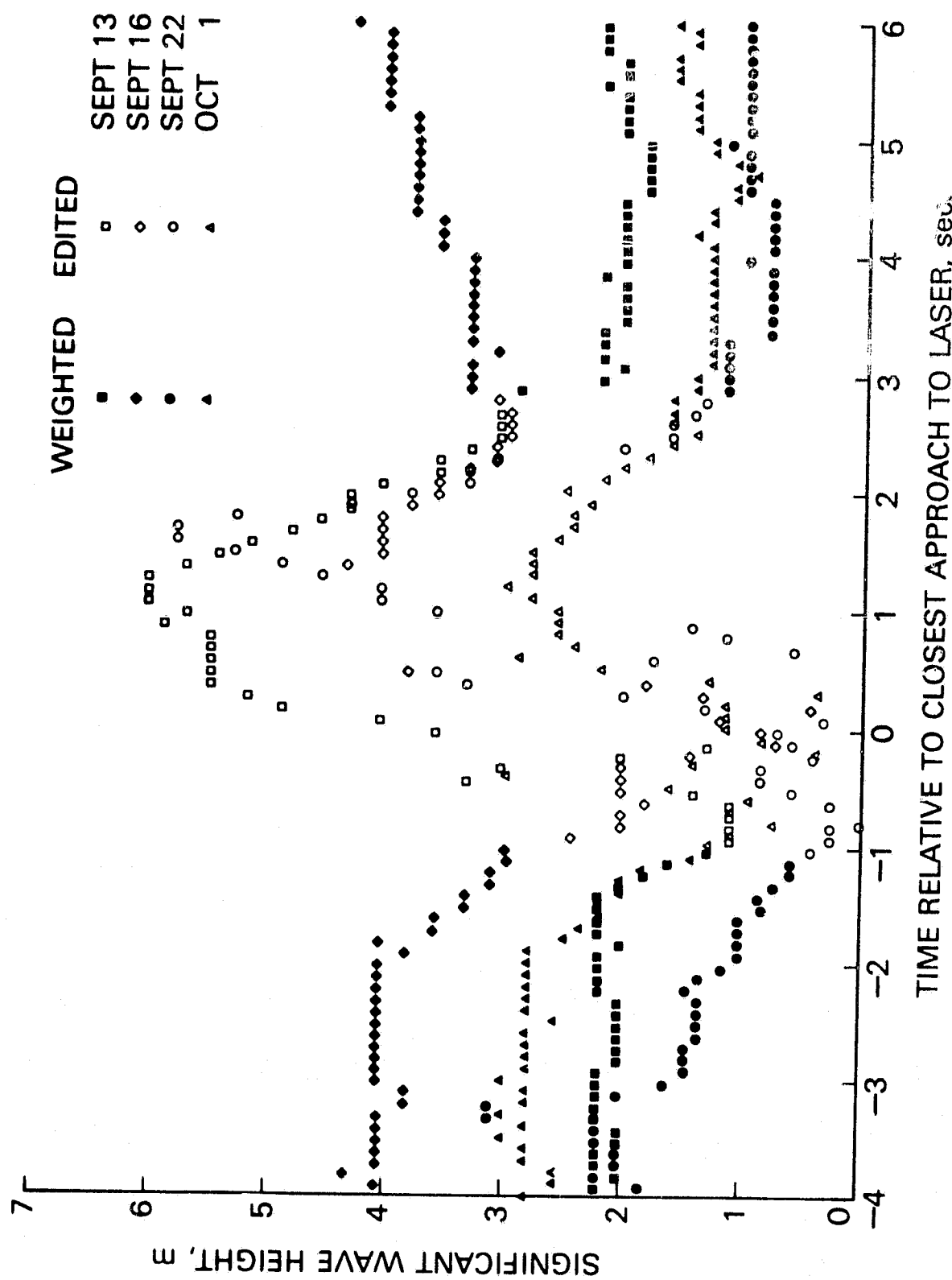


Fig. 5. Significant wave heights in the vicinity of Bermuda as computed from the altimeter data.

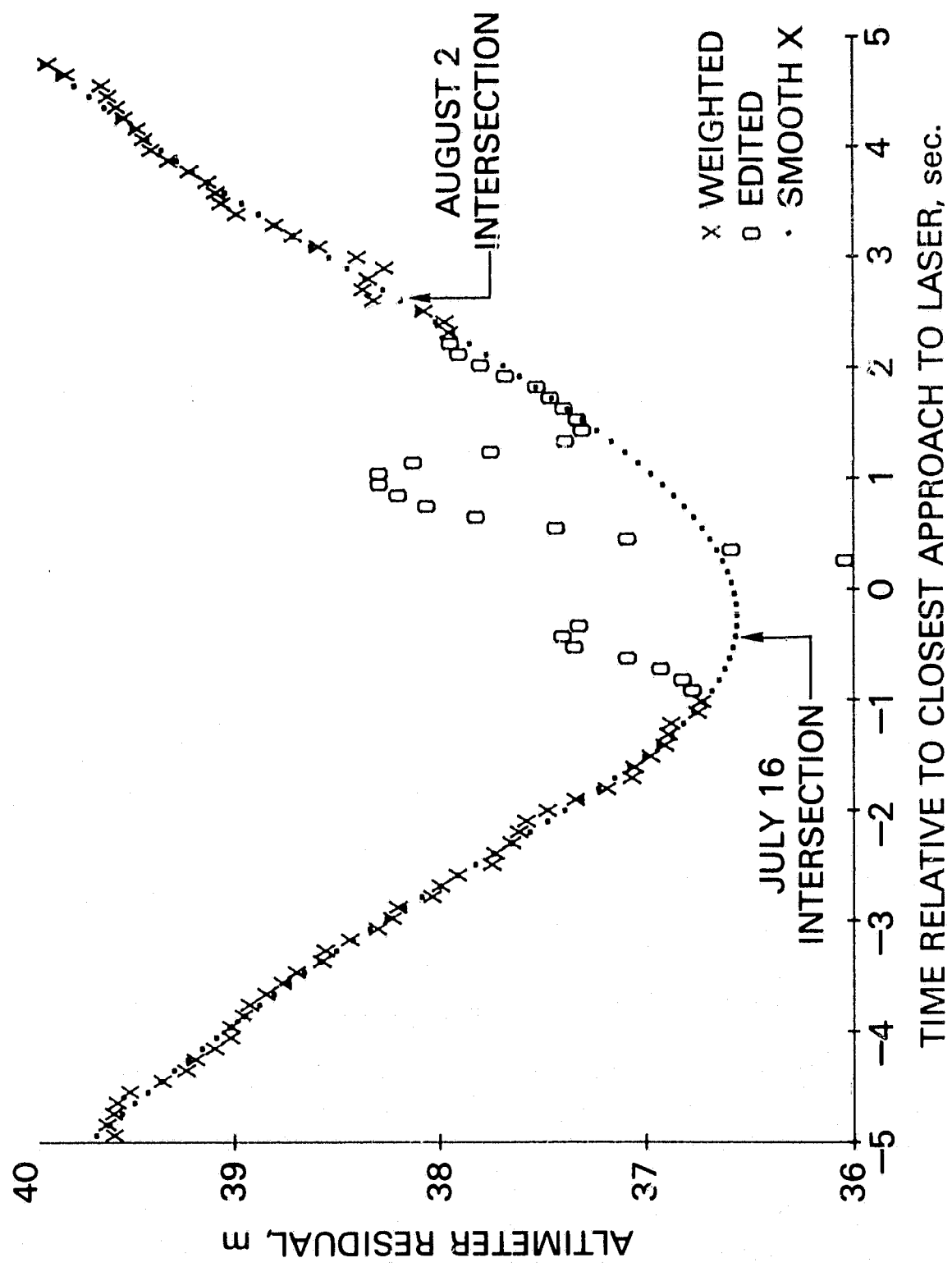


Fig. 6. Altimeter residuals for Seasat pass on September 13.

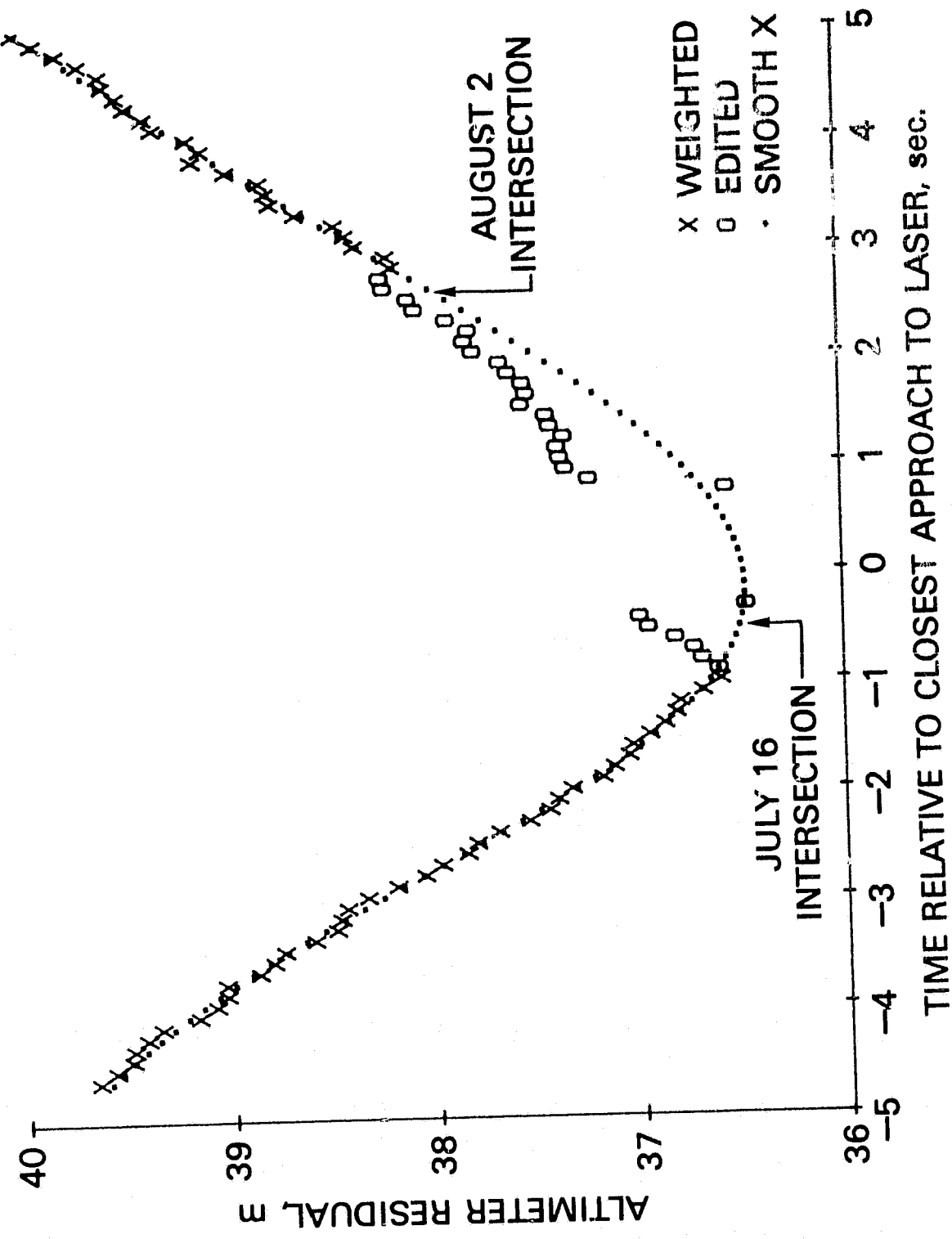


Fig. 7. Altimeter residuals for Seasat pass on September 16.

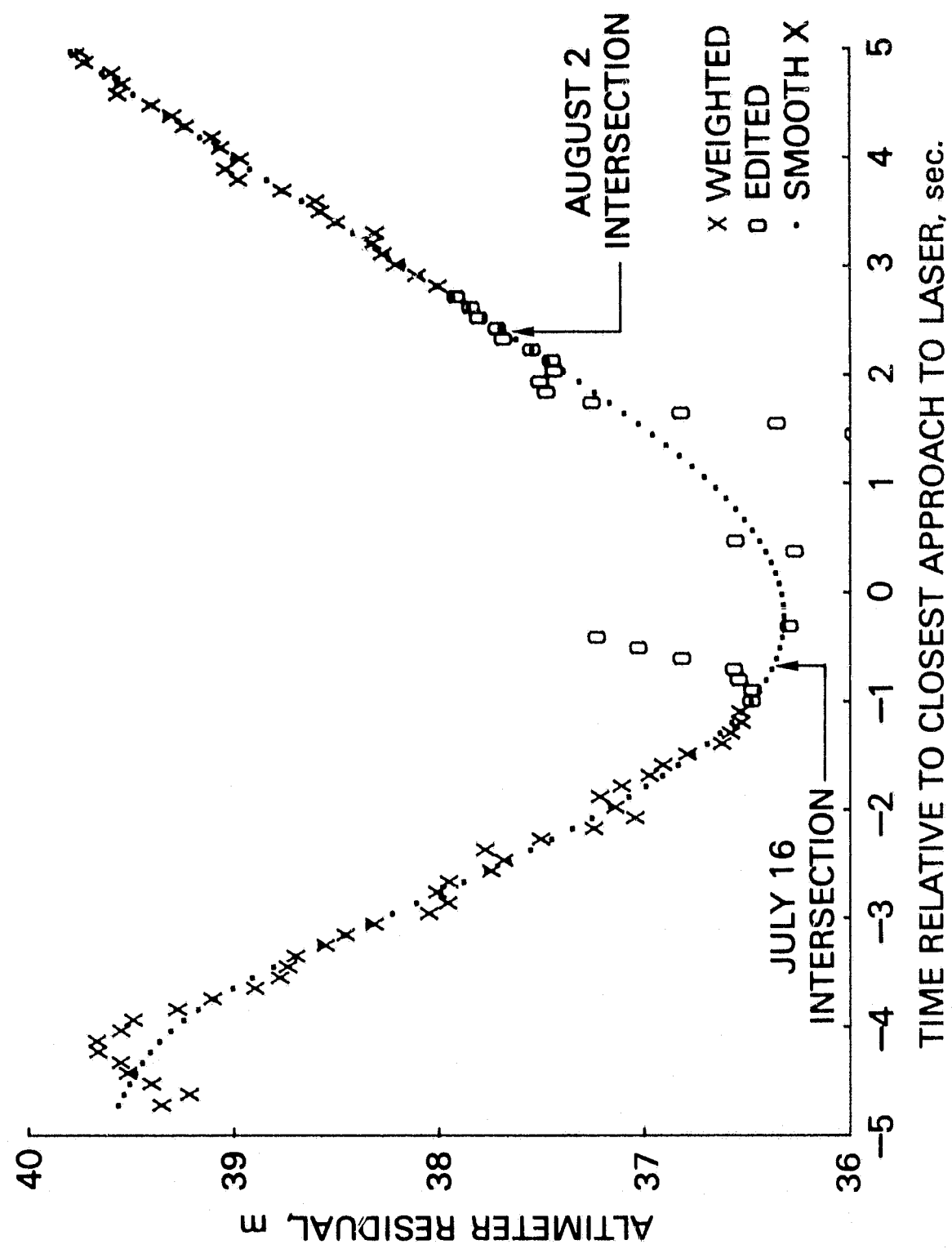


Fig. 8. Altimeter residuals for Seasat pass on September 22.

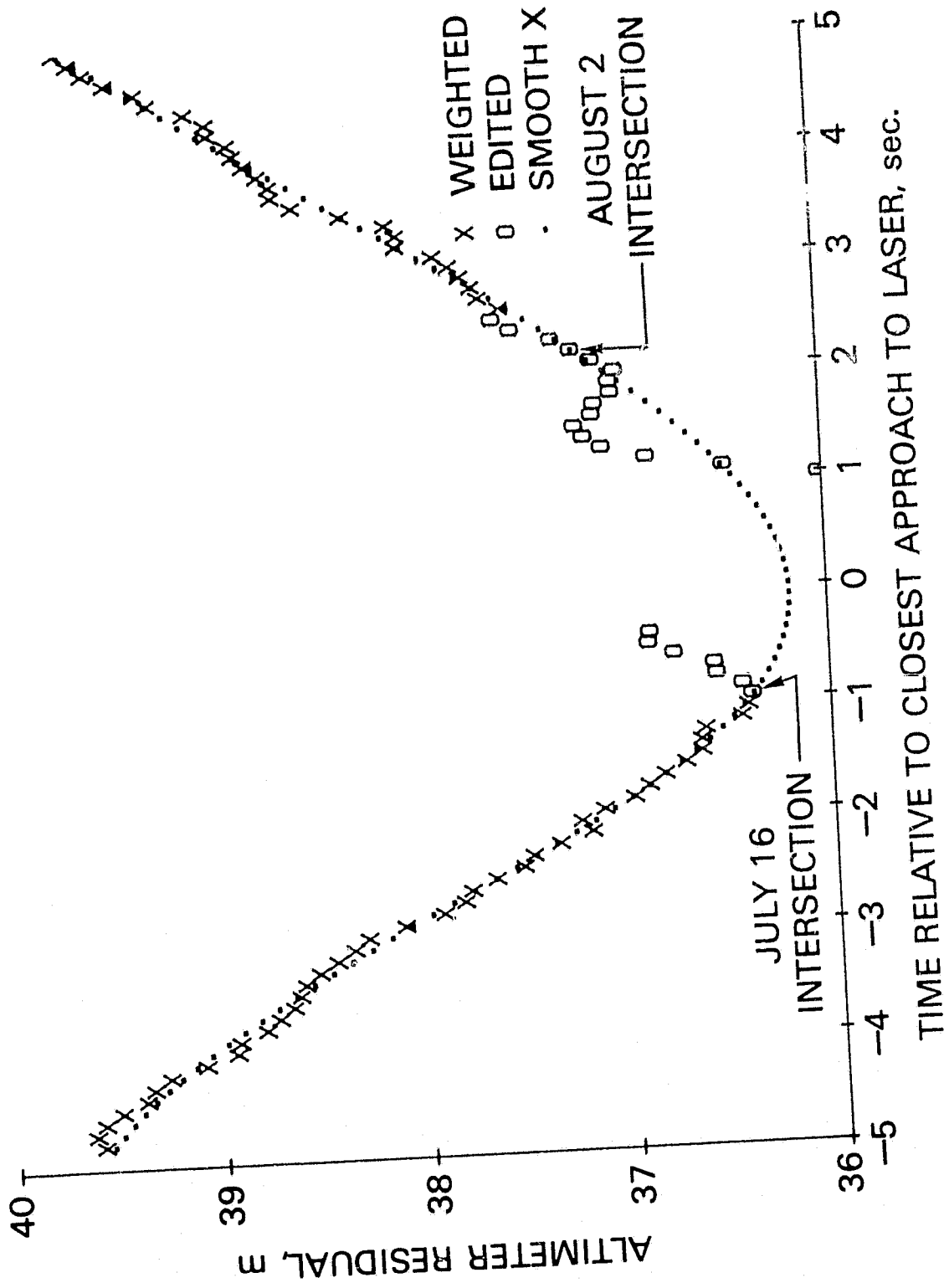


Fig. 9. Altimeter residuals for Seasat pass on October 1.

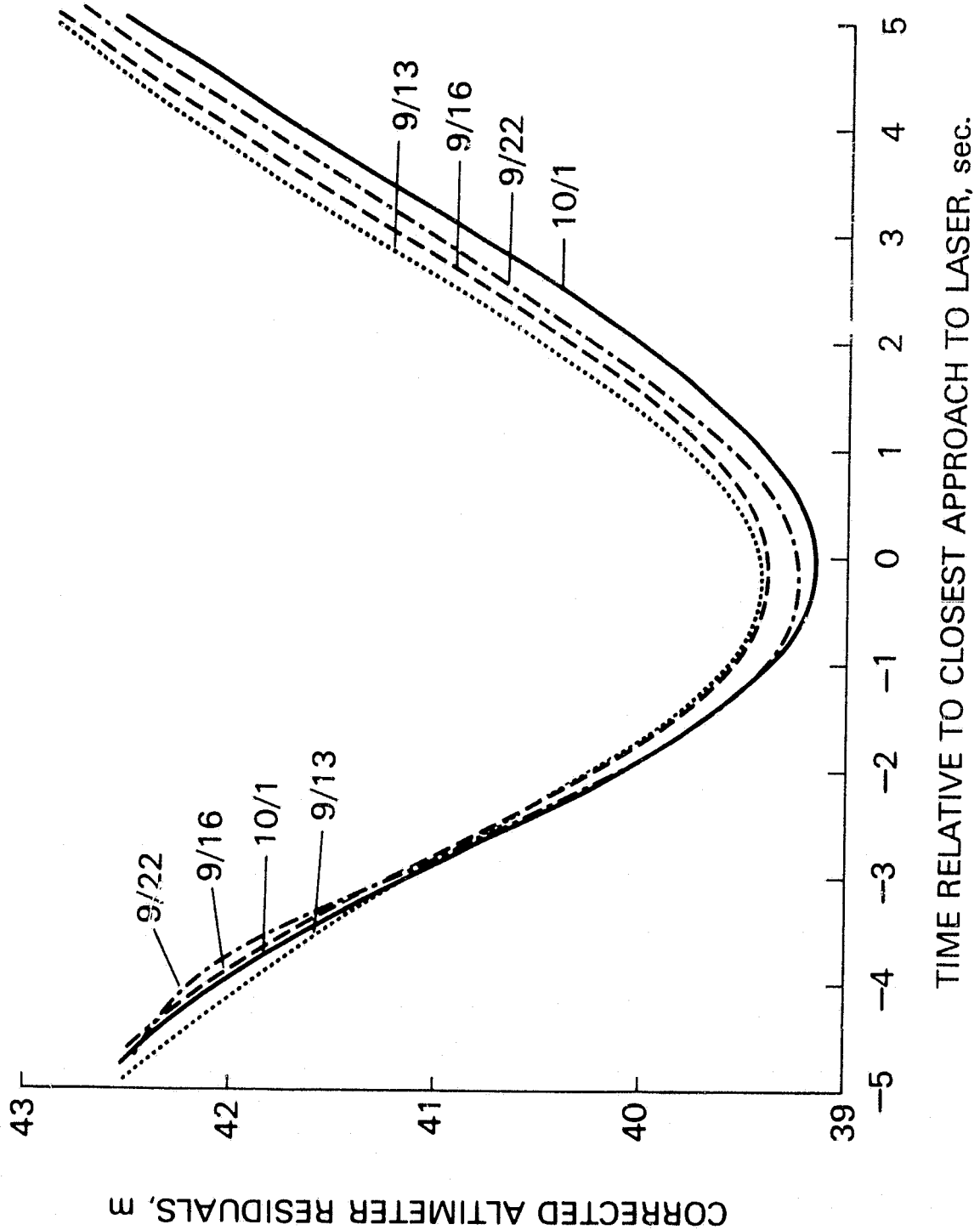


Fig. 10. Smoothed altimeter residual profiles across Bermuda. Corrections from Table 2 are included.

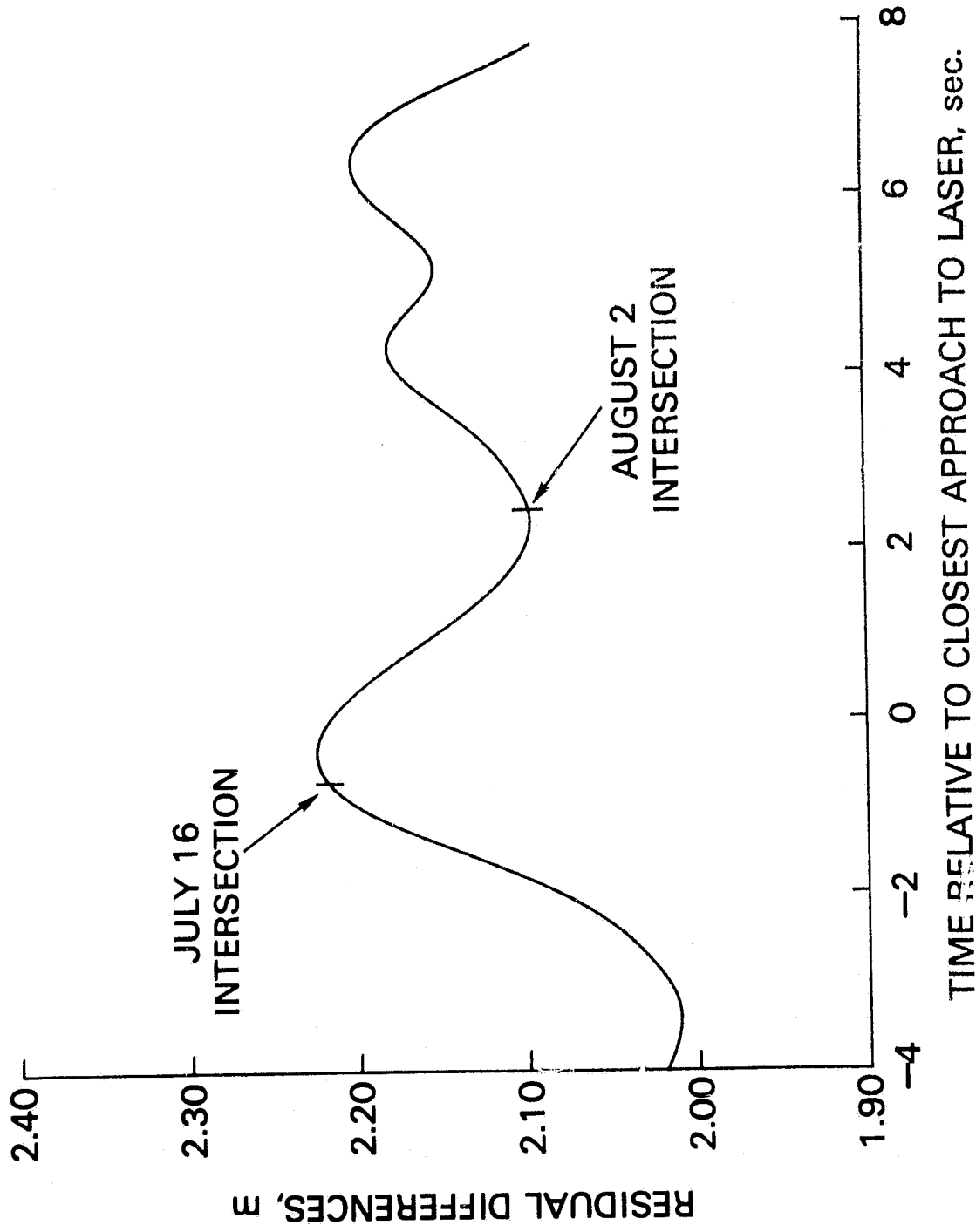


Fig. 11. Smoothed residual differences between overlapping passes October 4 minus October 1. RMS = 5.6 cm.

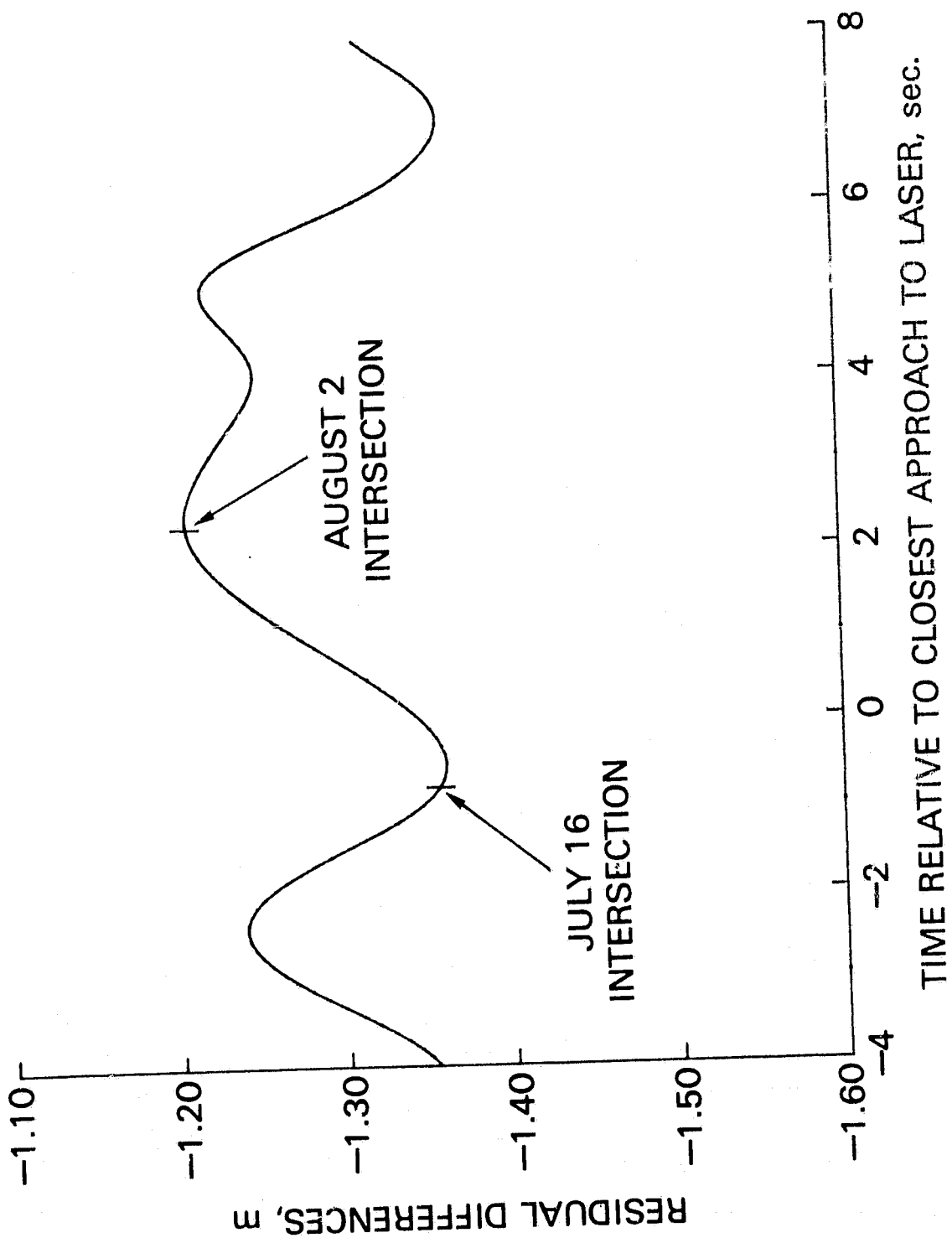


Fig. 12. Smoothed residual differences between overlapping passes September 28 minus October 4. RMS = 6.5 cm.

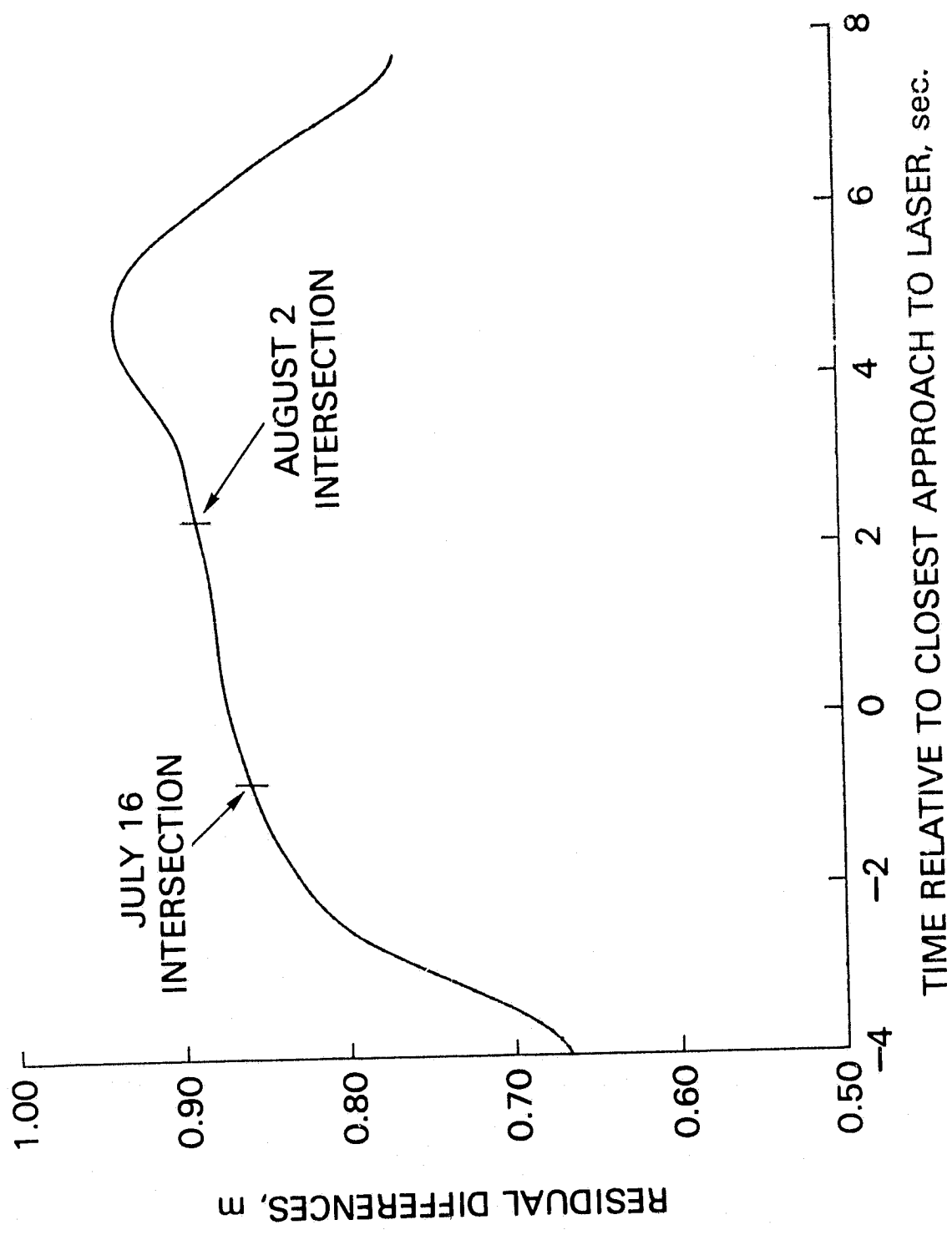


Fig. 13. Smoothed residual differences between overlapping passes September 28 minus October 1. RMS = 7.9 cm.

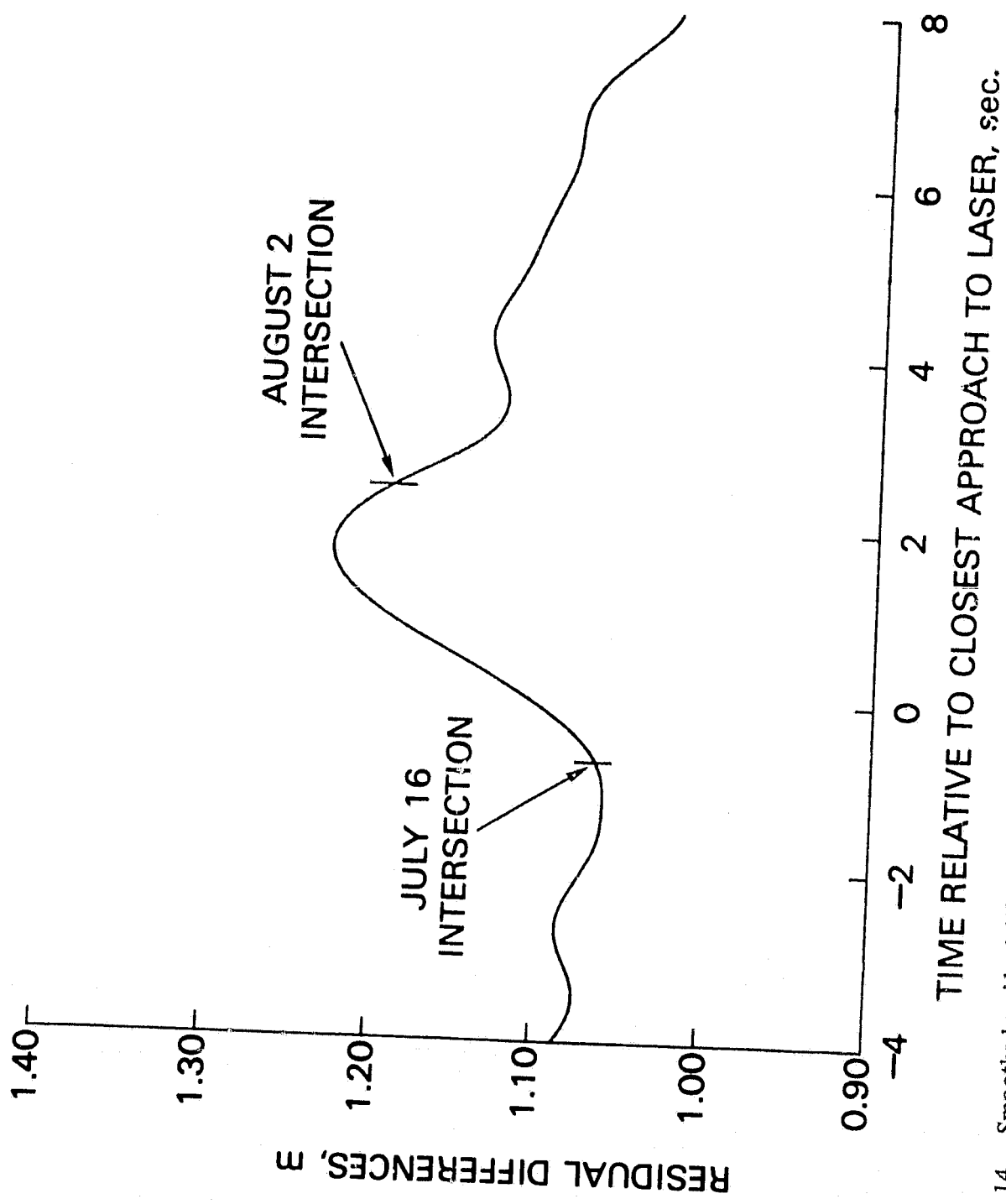


Fig. 14. Smoothed residual differences between overlapping passes September 25 minus October 7. RMS = 5.0 cm.

(7/16/78 9:17)

RMS OF FIT = 0.009 m

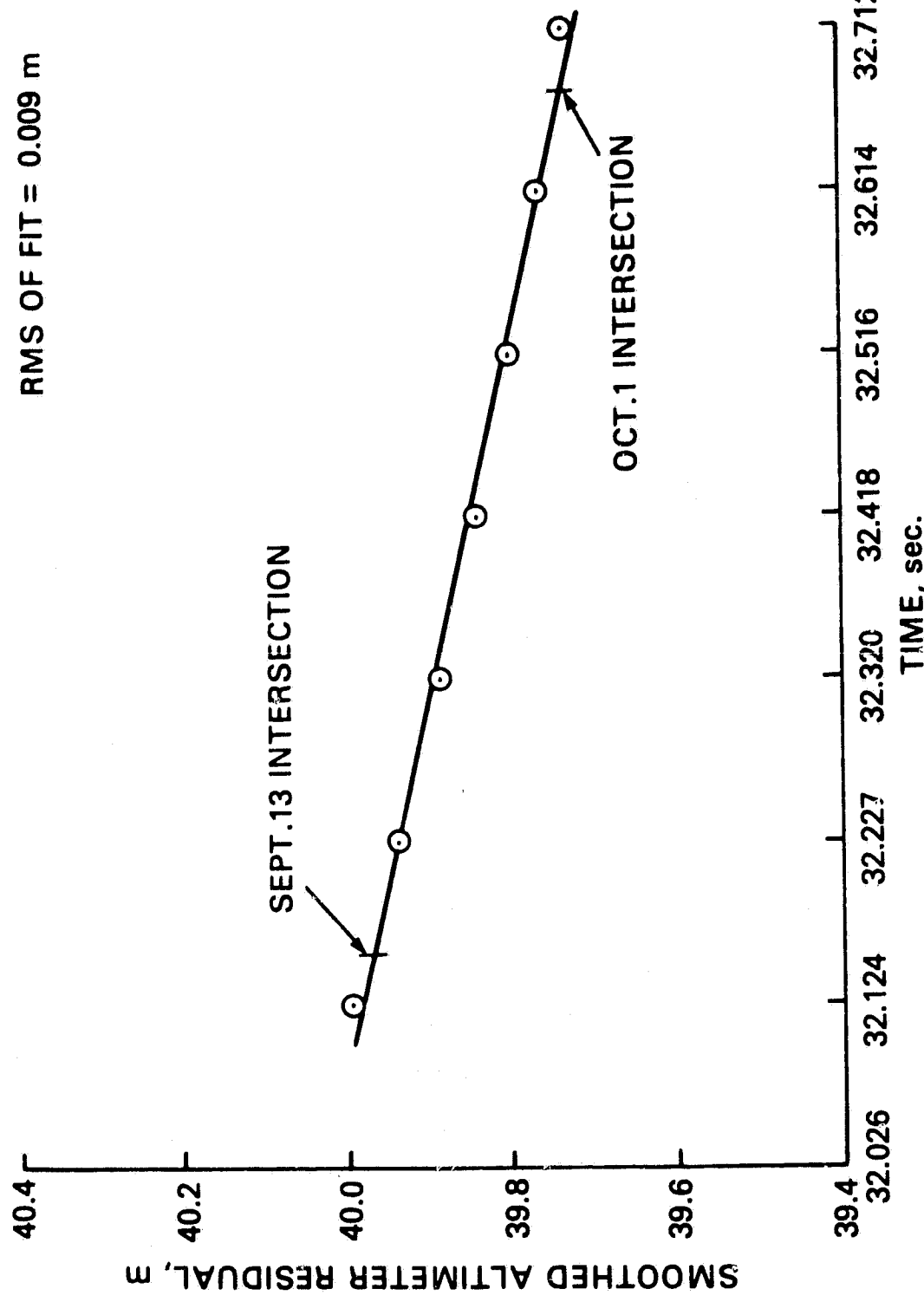


Fig. 15. Smoothed residual profile on July 16 south to north pass, showing linearity of geoid, transverse to the calibration passes.

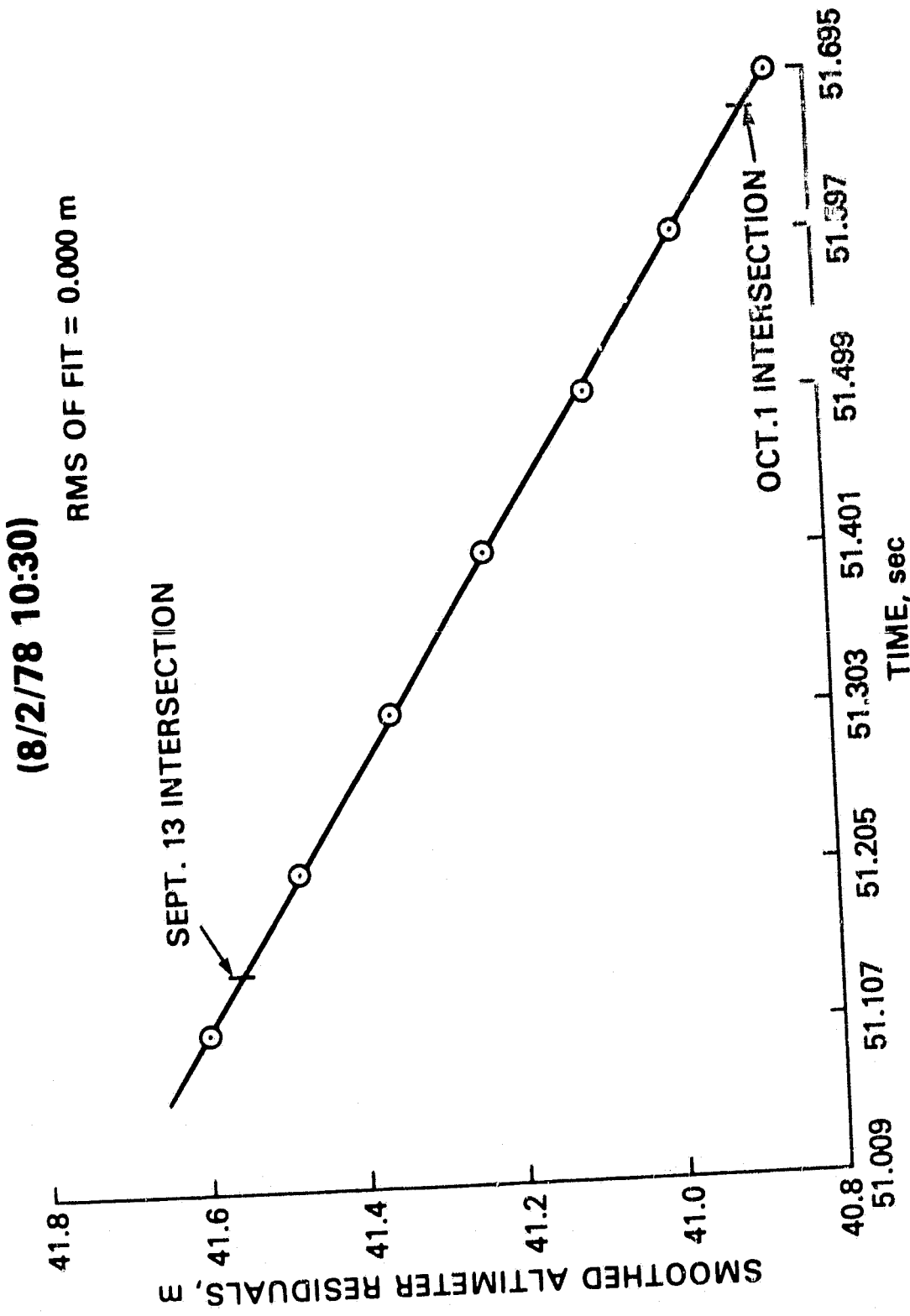


Fig. 16. Smoothed residual profile on August 2 south to north pass, showing linearity of geoid, transverse to the calibration passes.

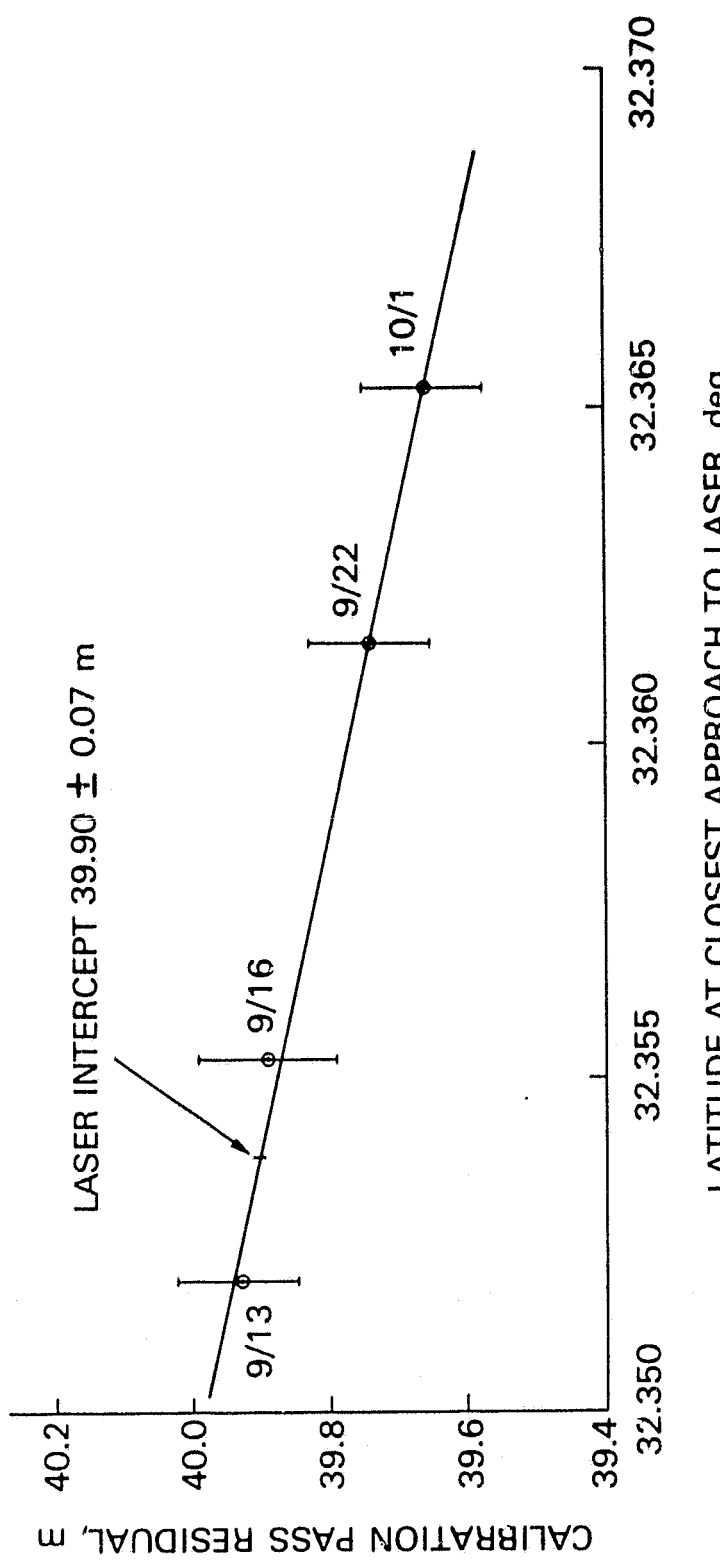


Fig. 17. Smoothed altimeter residuals at closest approach to laser.